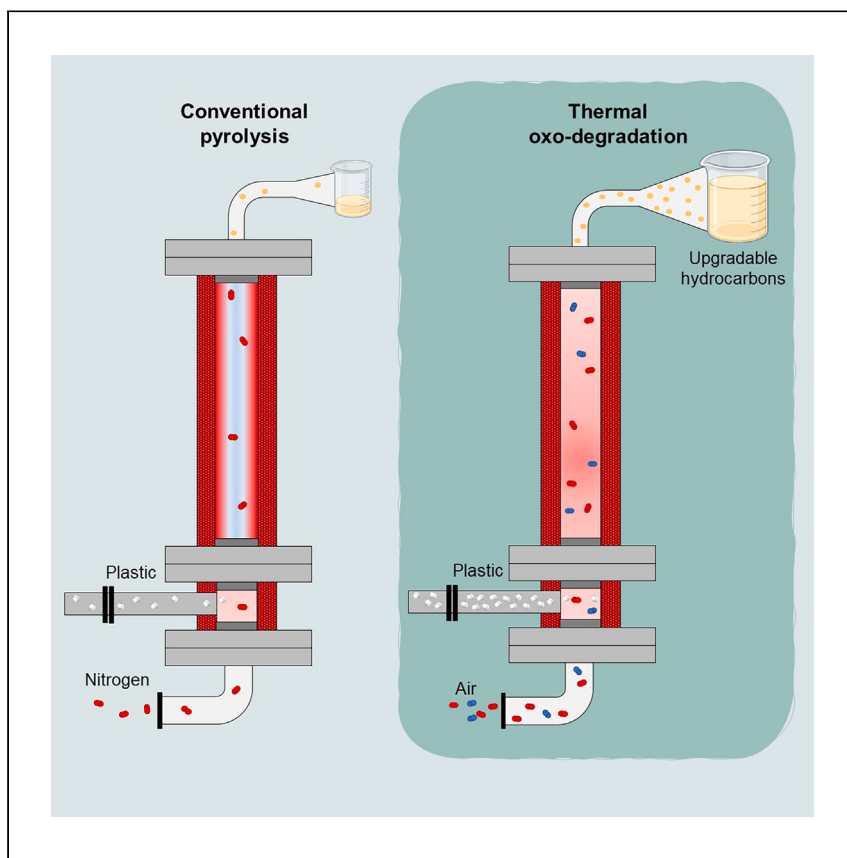


**Article**

# Increasing pyrolysis oil yields and decreasing energy consumption via thermal oxo-degradation of polyolefins



Thermal oxo-degradation is a form of oxidative pyrolysis used in the upgrading of plastics. Here, Brown et al. show that introduction of oxygen promotes partial oxidation of plastics, releasing heat in the reaction and decreasing external energy needs for hydrocarbon products that can be upgraded to monomers.

Jessica L. Brown, Robert C. Brown, Victor S. Cecon, Keith Vorst, Ryan G. Smith, Tannon J. Daugaard

daugaard@iastate.edu

## Highlights

Rapid plastic deconstruction using thermal oxo-degradation

Thermal oxo-degradation uses less external energy than pyrolysis

Hydrocarbon yields are preserved during thermal oxo-degradation



Article

# Increasing pyrolysis oil yields and decreasing energy consumption via thermal oxo-degradation of polyolefins

Jessica L. Brown,<sup>1</sup> Robert C. Brown,<sup>1,2</sup> Victor S. Cecon,<sup>3</sup> Keith Vorst,<sup>3</sup> Ryan G. Smith,<sup>2</sup> and Tannon J. Daugaard<sup>1,2,4,\*</sup>

## SUMMARY

Commercialization of pyrolysis of plastics in an inert atmosphere is challenging due to large thermal requirements. This study employs thermal oxo-degradation and demonstrates how oxygen supplied at modest equivalence ratios can both accelerate depolymerization and provide the enthalpy for pyrolysis without dramatically impacting desired product yields. The enthalpies for pyrolysis of high-density polyethylene (HDPE) and polypropylene (PP) are measured to be  $2,300 \pm 90 \text{ J g}^{-1}$  and  $2,800 \pm 60 \text{ J g}^{-1}$ , respectively. Using air as an oxygen source in a fluidized bed reactor, HDPE and PP are rapidly deconstructed while using up to 84% less energy through the energy released by partial oxidation. Characterization of the thermal oxo-degradation product oil shows comparable composition to conventional pyrolysis oil. Thermal oxo-degradation proves to be a promising technology for upcycling of plastics by improving thermal depolymerization of waste plastics and reducing energy requirements while maintaining desirable yields.

## INTRODUCTION

Lack of attention to the end-of-life disposal of plastics has resulted in their relentless accumulation in the environment, causing pollution and endangering natural and human-made environments. According to Geyer et al.,<sup>1</sup> 79% of all plastics ever produced reside in landfills or the environment, reflecting the low utility of plastic wastes. Although plastics slowly decompose in the natural environment, performance properties degrade with time, explaining in part the low rates of mechanical recycling of plastic. This issue has motivated research on upcycling, largely defined as depolymerizing plastics into chemical building blocks for new products.<sup>2</sup>

Polyethylene (PE) and polypropylene (PP) have been well established as feedstocks for upcycling.<sup>3</sup> Pyrolysis, defined as the thermal decomposition of polymers in an inert atmosphere, is one means of upcycling plastics to commodity chemicals and fuels.<sup>4,5</sup> The mechanism of plastics pyrolysis is a free-radical random-chain scission, breaking the polymer backbone into shorter fragments of variable length.<sup>6</sup> At moderate temperatures ( $<500^\circ\text{C}$ ) and short residence times ( $<1 \text{ s}$ ), long-chain polymers are cracked into predominantly C21 and larger molecules (wax), lesser amounts of C6-C20 molecules (oil), C5 and smaller molecules (gas), and solid carbonaceous residue (char).<sup>7,8</sup> Higher temperatures lead to increased yields of oil and gas.<sup>9</sup> Pyrolysis wax constitutes hydrocarbons of carbon lengths above C21<sup>3,10</sup> with applications as lubricant<sup>10</sup> or as a feedstock for fluidized catalytic cracking units.<sup>11</sup> Oil in the range of C6-C20 can be catalytically upgraded to small olefins for plastics manufacturing<sup>2,12</sup>

<sup>1</sup>Department of Mechanical Engineering, Iowa State University, Ames, IA 50011, USA

<sup>2</sup>Bioeconomy Institute, Iowa State University, Ames, IA 50011, USA

<sup>3</sup>Department of Food Science and Human Nutrition, Iowa State University, Ames, IA 50011, USA

<sup>4</sup>Lead contact

\*Correspondence: daugaard@iastate.edu

<https://doi.org/10.1016/j.xcpr.2024.101856>



or can serve as diesel fuel.<sup>13–15</sup> Despite extensive investigations of plastic pyrolysis, there are challenges to making the process commercially viable, including the relative difficulty of supplying large amounts of thermal energy to pyrolyzers.<sup>16,17</sup> While granular heat carriers can increase the energy efficiency,<sup>18</sup> this phenomenon is surface-area limited, and the heat transfer to the reactor can become a bottleneck as the reactor is scaled.<sup>19</sup>

Addition of oxygen to facilitate decomposition of plastics, referred to as “thermal oxo-degradation” (TOD), combines chain breaking and oxidation of polymers. Due to the addition of oxygen, lower devolatilization-onset temperatures of plastics pyrolysis are observed.<sup>20</sup> Similar to plastics pyrolysis, TOD proceeds through a multi-step free-radical chain reaction. Initiation of the reaction often occurs at weak links—impurities, hydroperoxides, and carbonyl groups—along the carbon chain that may have formed during the processing stage of the life cycle of the plastics.<sup>21</sup> Once these weak links have reacted, depolymerization becomes limited by the rate of random scission.<sup>20</sup> The reaction pathway to oxygenated molecules begins with the formation of peroxy radicals in the presence of diatomic oxygen. Hydrogen abstraction of peroxy radicals produces hydroperoxides. The extent of oxidation depends upon the reaction conditions. At more severe reaction conditions, hydroperoxides will decompose to carboxylic acids, alcohols, or aldehydes.<sup>22</sup> The products from TOD also include hydrocarbons, as some of the fragmented oligomers of the plastic will not oxidize because the equivalence ratio (ER) is usually very small: there is a deficit of oxygen compared to the amount of carbon and hydrogen in the plastic.<sup>23</sup>

TOD is distinct from air-blown or oxygen-blown gasification, despite the fact that both employ oxidation to help drive the process. Gasification is ideally driven to a state of chemical equilibrium, whereas TOD is a distinctly non-equilibrium process, with the former producing predominately non-condensable gases (NCGs) and the latter producing mostly condensable products. Relatively short vapor residence times during TOD is important to achieving high condensable product yield. TOD and gasification also have distinct operating conditions of temperature and ER (that is, the ratio of air used in the system to the stoichiometric air required for complete combustion). Gasification is typically operated between 800°C and 1,700°C, as higher temperatures favor a close approach to equilibrium, encouraging the production of gaseous products.<sup>2,4,24–26</sup> Gasification of plastics operates at ERs of 0.2–0.4.<sup>27</sup> In contrast, TOD operates at much lower ERs (<0.2) and more modest temperatures (400°C–600°C) to produce high liquid yields and minimize oxidation to NCGs (CO, CO<sub>2</sub>, and H<sub>2</sub>O).<sup>23</sup> Some researchers purportedly studying gasification of plastics appear to have been operating at reaction conditions more typical of TOD and produced significant condensable products, as expected from TOD. For example, Mastral et al.<sup>28</sup> performed thermal degradation of high-density PE (HDPE) in both nitrogen and nitrogen-air mixtures using a fluidized bed, which they designated as gasification. However, the ERs of these experiments were only 0.06–0.07, and the products included significant amounts of wax and liquid (condensate), as expected for TOD. In tests conducted in the nitrogen-air mixtures, organic products included both hydrocarbons and oxygenated compounds.<sup>28</sup>

TOD of plastic helps overcome a primary disadvantage of pyrolysis, which is the large amount of energy required to drive endothermic cracking of polymer chains. A similar concept, known as autothermal pyrolysis, has been extensively studied for biomass feedstock.<sup>29</sup> Polin et al.<sup>30</sup> showed that exothermic oxidation reactions during autothermal pyrolysis provided enough energy to overcome the enthalpy

for pyrolysis of biomass, eliminating the need for external heat. In TOD of plastics, partial oxidation reactions are also exothermic, providing some of the energy needed to crack polymer chains and decreasing the need to externally provide thermal energy to the process.<sup>19</sup> As the energy demand for pyrolysis increases volumetrically with more throughput, internal partial oxidation allows easier scale-up as the process becomes chemical kinetically limited as opposed to heat transfer limited.<sup>19</sup> The present study investigates energy flows during conventional pyrolysis and TOD of select plastics.

The enthalpy associated with plastics pyrolysis has been extensively studied using benchtop systems; however, differences between methodologies have led to a wide range of reported values. Distinguishing between "enthalpy of pyrolysis" and "enthalpy for pyrolysis" is important. The summation of sensible enthalpy, enthalpy of melting, and enthalpy of pyrolysis is what Daugaard and Brown referred to as enthalpy for pyrolysis.<sup>31</sup> Other researchers studied only the enthalpy of pyrolysis, which is the energy required to drive the cracking and volatilization reactions of pyrolysis. Duque et al.<sup>32</sup> used simultaneous thermal gravimetric analysis/differential scanning calorimetry (TGA/DSC) and reported enthalpies of pyrolysis of 299 and 205 J g<sup>-1</sup> for virgin and recycled low-density PE (LDPE), respectively, suggesting significant differences even within a class of polymers. These values are low compared to the reported enthalpy of pyrolysis of 920 ± 120 J g<sup>-1</sup> for virgin PE for Khedri et al.<sup>33</sup> In the study by Khedri et al.,<sup>33</sup> the authors accounted for heat loss during DSC and integrated apparent and sensible specific heat curves to calculate the enthalpies, but this methodology was later claimed to be mathematically incorrect by other researchers.<sup>34</sup>

Agarwal and Lattimer<sup>34</sup> developed a method for measuring the standard enthalpy of decomposition of materials using simultaneous TGA/DSC. Their measurement greatly improved upon the typical approaches by accounting for the heat capacity of gases leaving the crucible. In addition, their method of measuring the energy required to vaporize volatile material from the solid was more accurate for determining the enthalpy for pyrolysis. Agarwal and Lattimer's experimentally determined enthalpies for pyrolysis of HDPE (molecular weight [MW] = 125,000 Da), LDPE (MW = 35,000 Da), and PP (MW = 12,000 Da) were 1,940.9, 1,870, and 1,684.8 J g<sup>-1</sup>, respectively.<sup>34</sup> However, the gas composition used to calculate the heat capacity of gases leaving the crucible was taken from a study of catalytic pyrolysis of HDPE. While a catalyst does not affect the change in enthalpy of a chemical reaction, its use enhances selectivity toward low-MW products in plastic pyrolysis. In Elordi's study of catalytic pyrolysis,<sup>35</sup> the products were mostly in the range of C5–C10, with only 2.06 wt % of the product molecules having chain lengths greater than C12. As molar heat capacity generally increases with MW, using this dataset would result in a lower heat capacity, which would result in a lower enthalpy for pyrolysis. Furthermore, benchtop systems (like the TGA) can have heat and mass transfer limitations compared to fluidized beds as used in the present study. Thus, most experimental methods have underestimated the enthalpy for plastic pyrolysis, a key parameter for evaluating economic viability of a commercial plant.<sup>36</sup>

The first objective of this study is to quantify the energy consumption during conventional pyrolysis and TOD of plastics. We propose using a continuous fluidized bed reactor as a method of obtaining accurate values of enthalpy for pyrolysis of plastics. A methodology similar to one previously used in studies of biomass pyrolysis<sup>31</sup> will be employed to determine the enthalpy for pyrolysis of virgin HDPE and PP plastics.

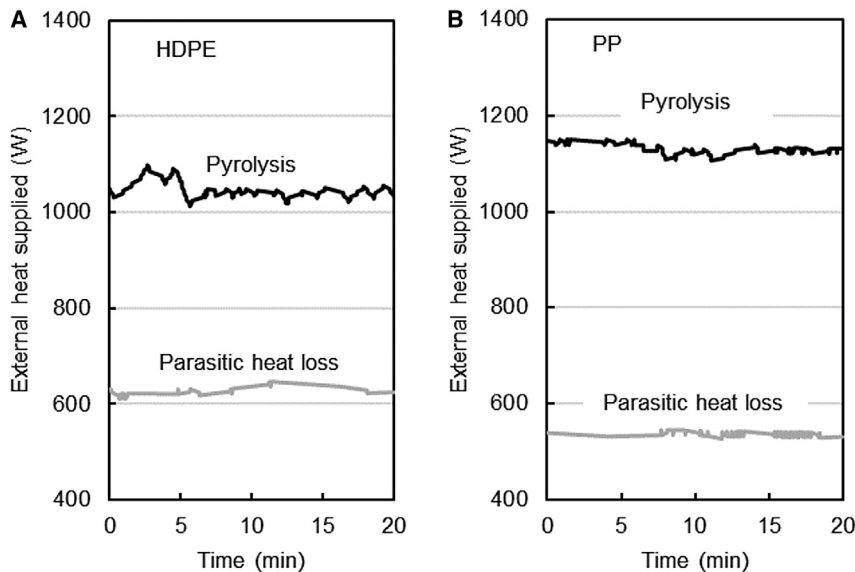


**Figure 1. Reactor heater power during pyrolysis**

Heater power during operation of pyrolysis at 600°C with (A) HDPE and (B) PP. The power for the heaters to overcome parasitic heat loss to the surrounding environment is also displayed.

This method is also used to evaluate the exothermic heat released during partial oxidation of TOD at two ERs.

The second objective of this study is to characterize the products of TOD. Typically, it is desired to exclude oxygen from thermal decomposition of plastics to maximize liquid hydrocarbon output. However, in low concentrations, oxygen can catalytically enhance pyrolysis cracking reactions while producing the majority of hydrocarbons.<sup>37</sup> The present study evaluates the effectiveness of TOD to preserve hydrocarbon yields through carefully controlled conditions of temperature, ER, and oxygen concentration.

## RESULTS AND DISCUSSION

### Determination of enthalpy for pyrolysis

Figure 1 illustrates how parasitic heat losses and the addition of oxygen influence the demand for external thermal energy to maintain the reactor temperature at 600°C. The difference between average energy demand during pyrolysis and the parasitic heat losses divided by the feed rate of plastics into the reactor gives the enthalpies for pyrolysis, which are  $2,300 \pm 90$  and  $2,800 \pm 60$  J g<sup>-1</sup> (for HDPE and PP, respectively).

The enthalpy for pyrolysis of HDPE was determined in this work to be  $2,300 \pm 90$  J g<sup>-1</sup>, which includes total energy consumed to converted solid feedstock into reactants, including sensible enthalpy, heat of melting, and reaction enthalpy. This value can be compared with the theoretical value of 2,800 J g<sup>-1</sup> presented by Dispens,<sup>38</sup> who posited that of the 2,800 J g<sup>-1</sup> required for enthalpy for polyolefin plastic pyrolysis, 2,200 J g<sup>-1</sup> is required to break seven carbon–carbon bonds per kg of polymer to produce the hydrocarbon vapors. The remaining 600 J g<sup>-1</sup> is due to sensible enthalpy and heat of melting. The 18% lower value measured in the present experiments are thought to be due to inadvertent preheating of the plastic in the feed auger, which is in thermal contact with the hot fluidized bed reactor. The determined enthalpy for pyrolysis of PP was  $2,800 \pm 90$  J g<sup>-1</sup>. Partial melting of PP feedstock was

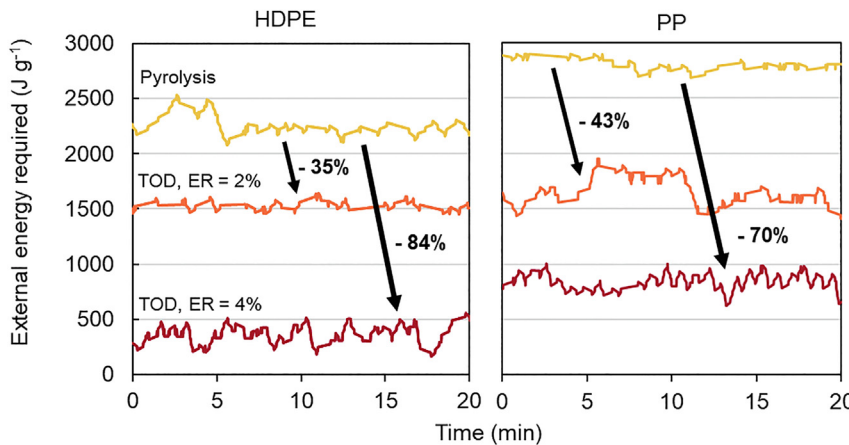


**Figure 2. Decrease in TOD energy external energy**

External thermal energy demand during TOD reactions (ER = 2%, ER = 4%) is plotted against the external energy demand for pyrolysis. Bold values accompanied with arrows indicate percentage of decrease in external energy demand.

also observed in the feed auger. The higher enthalpy for pyrolysis of PP can possibly be attributed to the larger MW of the PP feedstock (MW = 270,000 Da) over the HDPE feedstock (MW = 65,000 Da), requiring eight carbon–carbon bonds per kg of polymer to be broken to generate volatile compounds at reactor temperatures.

The enthalpy for pyrolysis values observed in the current investigation are on the same order of magnitude as those experimentally determined using TGA/DSC by Agarwal and Lattimer,<sup>34</sup> who accounted for sensible enthalpy, heat of melting, and reaction enthalpy. Other studies only account for reaction enthalpy, which is referred to as enthalpy of pyrolysis.<sup>32,33</sup> It is important to distinguish between enthalpy of pyrolysis and enthalpy for pyrolysis when comparing results of different researchers. As the required reaction energy has a major influence on pyrolysis reactor design, it is important to use the correct enthalpy for pyrolysis when designing a system. Improper usage of enthalpies for pyrolysis can result in underestimation of capital and operating costs and potentially insufficient heat allotment. The use of a continuous reactor system in the determination of enthalpy for pyrolysis, as demonstrated in this work, better approximates the conditions required for the upcycling of plastic at scale.

#### Decrease in external thermal energy demand during TOD

As air was introduced to the system for TOD experiments, the exothermic partial oxidation reactions of TOD released heat internally, providing some of the enthalpy for the endothermic carbon bond cracking reactions. Therefore, less external heat from the heaters was needed to maintain reaction temperatures (Figure 2). The external energies required for HDPE TOD reactions were  $1,500 \pm 30$  and  $360 \pm 90$  J g<sup>-1</sup>, 35% and 84% decreases, respectively, from the enthalpy for pyrolysis in an adiabatic reactor. The external energies required for PP TOD reactions were  $1,600 \pm 30$  and  $830 \pm 70$  J g<sup>-1</sup>, 43% and 70% decreases, respectively, from the enthalpy for pyrolysis of an adiabatic reactor. The decrease in external heat required to sustain reaction conditions is a result of the partial oxidation reactions during TOD operation. Table 1 summarizes these results.

#### Comparison of product distribution between pyrolysis and TOD

The yields of wax, liquid, and NCGs for pyrolysis and TOD tests are displayed for HDPE and PP in Figure 3. No char was produced from pyrolysis of these pure

**Table 1. Calculated enthalpy values**

	HDPE	PP
Enthalpy for pyrolysis ( $\text{J g}^{-1}$ )	$2,300 \pm 90$	$2,800 \pm 60$
External energy demand for TOD, ER = 2% ( $\text{J g}^{-1}$ )	$1,500 \pm 30$	$1,600 \pm 100$
External energy demand for TOD, ER = 4% ( $\text{J g}^{-1}$ )	$360 \pm 90$	$830 \pm 70$

Calculated enthalpy values ( $\text{J g}^{-1}$ ) for pyrolysis and external energy required for thermal o xo-degradation (TOD) with equivalence ratios of 2% and 4%. Also denoted is the percentage of reduction in external energy demand during TOD. Virgin high-density polyethylene (HDPE) and polypropylene (PP) were used as feedstock. Error is determined by standard deviation of heater powers throughout the duration of the tests.

polymers. Liquid yield is separately reported for the oil and aqueous phases (for TOD tests). NCGs are separated into light gases (LGs) and carbon oxides ( $\text{CO} + \text{CO}_2$ ). Figures S2 and S3 detail the composition of NCG yields for pyrolysis and TOD trials. Wax production was favored over liquid production in all tests, which is supported by other studies using reactors with short vapor residence times and rapid quenching.<sup>39–41</sup> For pyrolysis of HDPE at 600°C, the wax average yield was 82 wt %, while oil and gas yields were 3 and 6 wt %, respectively. Pyrolysis of PP under identical conditions produced less wax (61 wt %) and more oil (16 wt %) and gas (13 wt %). The lower wax yield and higher oil yield for PP result from the higher susceptibility of tertiary carbon bonds in its branched chains to cracking than the double-bonded carbon atoms in the backbone of the HDPE chain.<sup>42,43</sup>

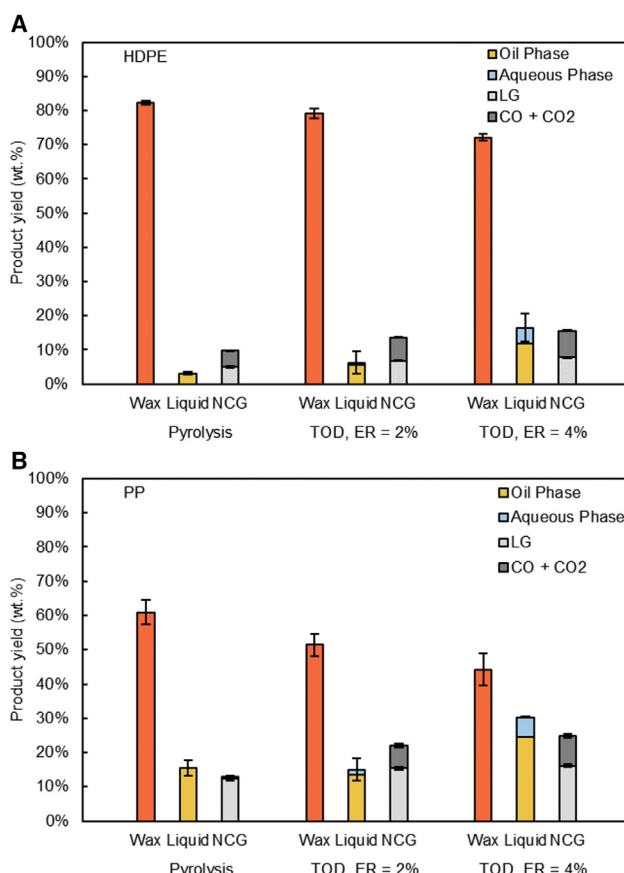


**Figure 3. Pyrolysis and TOD yields**

The yields of pyrolysis, TOD at ER = 2%, and TOD at ER = 4% for high-density polyethylene (A) and polypropylene (B). Error bars represent standard deviation of two trials around the average yields. Light gases are represented by "LG."

For both HDPE and PP feedstocks, the product distribution shifted toward oil when air was added to the reactor. TOD of HDPE for an ER of 2% still favored wax production, but its yield decreased to 80 wt % compared to pyrolysis, while both the oil and gas yields increased. This shift became more dramatic as ER increased to 4%. The trend of increased oil and gas yields during TOD is attributed to the reaction acceleration of oxygen on carbon cracking, first described by Mayo.<sup>37</sup> Even in small amounts, the addition of oxygen accelerates the rate of thermal decomposition.<sup>44</sup> Polymer degradation follows the elemental reaction steps of initiation, propagation, and termination, of which the radical initiation reactions have the highest activation energy.<sup>45</sup> When injected into the reaction, oxygen radicals increase the concentration of initiators.<sup>21</sup> Previous studies observed a significant decrease in the activation energy of homolytic cracking of carbon–carbon bonds in an oxidative environment compared to an inert environment.<sup>20,46</sup> According to Arrhenius theory, the reaction rate increases when the activation energy is lowered. Therefore, bonds are broken at faster rates in TOD than in pyrolysis, and a portion of the high-MW primary products are converted into liquid and gas.

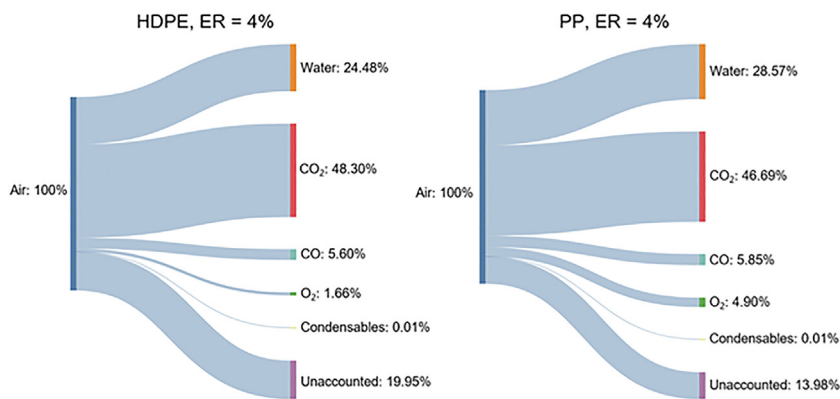
TOD experiments at both ER = 2% and 4% produced water and thus an aqueous phase along with other products, which naturally phase separated from the oil phase upon collection.<sup>28</sup> Karl Fischer titrations determined that water production from TOD of HDPE and PP did not exceed 3 and 3.9 wt %, respectively. The higher water content from PP over HDPE was expected, as thermal oxidation is initiated more rapidly at unhindered tertiary carbon atoms.<sup>44</sup> While the aqueous phase was primarily water (60–80 wt %), gas chromatography-mass spectrometry (GC-MS) analysis of the aqueous phase detected water-soluble oxygenated compounds that comprised the remainder of the aqueous phase, including light acids and phenolics. Hydroperoxides generated by the free-radical pairing reaction with available oxygen decomposed to carbonyl- and hydroxyl-containing groups,<sup>21,23,44</sup> which phase separated into the aqueous phase.

The main components of the light gases (LGs) of pyrolysis were ethylene, propane, propylene, and butene (see [supplemental information](#)). Lesser amounts of methane, ethane, and hydrogen were obtained. When air was introduced into the fluidizing gas for TOD conditions, the production of carbon oxides increased, as expected, where CO<sub>2</sub> was observed in higher concentrations than CO. The exothermic nature of partial oxidation reactions contributed to the internal energy for TOD reactions, as mentioned previously in the results. The fate of oxygen through TOD processing of HDPE and PP at ER = 4% is illustrated in [Figure 4](#). A portion of oxygen remains unaccounted for in each run, as the micro-GC was not calibrated for light oxygenated compounds that may not be collected as condensables. Additionally, water-soluble compounds in the aqueous phase were not included in the mass flows of oxygen.

Strikingly, only a small portion of feedstock carbon was sacrificed to provide the energy for TOD reactions, calculated by the weight of carbon converted into CO and CO<sub>2</sub>. TOD of HDPE and PP at ER = 4% converted only 2.9 and 2.6 wt % of the feedstock carbon, respectively, into CO and CO<sub>2</sub>. Based on their higher heating values (HHVs), the amounts of carbon in the plastics that would have to be theoretically oxidized to provide the enthalpy for pyrolysis and yield CO<sub>2</sub> and H<sub>2</sub>O would be 4.9 and 5.5 wt % for HDPE and PP, respectively.

#### Product wax characterization

Thermal depolymerization of polyolefins produces mostly wax as a primary product under short vapor residence times (<1 s). Such wax typically contains aliphatic

**Figure 4. Oxygen mass flows**

Mass flows of oxygen in TOD (ER = 4%) of HDPE (left) and PP (right). Condensables are comprised of wax and oil.

hydrocarbons of long chain length.<sup>41,47,48</sup> Elemental analysis showed an undetectable amount of oxygen in the waxes produced from both pyrolysis and TOD of HDPE and PP (Table 2). The carbon and hydrogen contents of all waxes were 85–86 and 14–15 wt %, respectively. The MWs and MW distribution for each product wax were measured to understand the impact of oxygen addition on thermal depolymerization. The waxes produced from TOD demonstrated lower number-average MW ( $M_n$ ) and weight-average MW ( $M_w$ ) compared to the waxes produced from pyrolysis. These trends suggest that TOD can be effective in shifting the products of polyolefin depolymerization to lower-MW compounds without significant oxygen appearing in the products.

Waxes from pyrolysis of HDPE showed a  $M_w$  of 668 g mol<sup>-1</sup>. By determining the  $M_w$  of pyrolysis oils from GC-MS/flame ionization detector (FID) characterization and using wax and oil yields, the  $M_w$  of total condensable products from pyrolysis was calculated to be 558 g mol<sup>-1</sup>. HDPE feedstock possessed a  $M_w$  of 65,000 g mol<sup>-1</sup>. The carbon–carbon bond in the central position on a hydrocarbon chain has the greatest tendency for cracking.<sup>49</sup> Cracking the central carbon–carbon bond of the starting polymer and those for the subsequent six product oligomers would theoretically produce hydrocarbon vapors with a  $M_w$  of 507 g mol<sup>-1</sup>, which is on the same order of magnitude of the experimentally determined  $M_w$  of total condensable products from pyrolysis. Furthermore, as the average bond dissociation energy of carbon–carbon bonds is 313 kJ mol<sup>-1</sup>, cracking seven carbon–carbon bonds per polymer kilogram gives a theoretical enthalpy for pyrolysis of 2,191 kJ kg<sup>-1</sup>.<sup>38</sup> Thus, the MW distribution from condensed pyrolysis products supports the experimentally determined enthalpy for pyrolysis presented in the section [determination of enthalpy for pyrolysis](#).

The calorific content of waxes did not change significantly with reaction conditions, as assessed by one-way ANOVA. The HHVs were found to be within the range of 45–46 MJ kg<sup>-1</sup> for all wax products, comparable to commercial heating oils. These values agree with the calorific values of HDPE and LDPE waxes found by Al-Salem and Dutta.<sup>47</sup> As demonstrated, TOD waxes have the same applications as pyrolysis waxes due to similarities in HHVs and elemental composition.<sup>50</sup> In fact, higher-MW wax fractions are avoided as feedstock for certain processes such as steam cracking due to their tendency to form coke.<sup>49</sup> The ability of TOD to shift the distribution of waxes toward lower MWs improves the application outlook of plastic-derived waxes.

**Table 2. Characteristics of TOD and pyrolysis waxes**

Feedstock	C (wt %)	H (wt %)	O (wt %)	$M_n$ (g mol $^{-1}$ )	$M_w$ (g mol $^{-1}$ )	HHV (MJ kg $^{-1}$ )
<b>HDPE</b>						
Pyrolysis	85.6 ± 0.1	14.4 ± 0.1	<0.01	442	668	45.8 ± 0.8
TOD, ER = 2%	85.4 ± 0.1	14.1 ± 0.3	<0.01	384	573	45.3 ± 0.2
TOD, ER = 4%	85.3 ± 0.1	14.3 ± 0.1	<0.01	320	498	45.5 ± 0.3
<b>PP</b>						
Pyrolysis	85.5 ± 0.1	14.0 ± 0.3	<0.01	599	920	45.7 ± 0.4
TOD, ER = 2%	85.4 ± 0.3	14.2 ± 0.1	<0.01	502	740	45.8 ± 0.8
TOD, ER = 4%	84.8 ± 0.6	14.1 ± 0.1	<0.01	451	702	45.4 ± 0.3

Ultimate analysis, higher heating values, and molecular weight for waxes obtained from pyrolysis and thermal oxo-degradation (TOD) at two equivalence ratios (ER) of high-density polyethylene (HDPE) and polypropylene (PP). Error for elemental analyses is represented by standard deviation of three trials around the average. Error for higher heating values (HHVs) is represented by standard deviation of two trials around the average.

### Product oil characterization

Olefins were more than 65 wt % of the oil produced from pyrolysis of HDPE (Figure 5). The concentrations of diolefins and paraffins in the oil were 16 and 15 wt %, respectively. The high concentration of olefin is consistent with other studies of HDPE pyrolysis oils.<sup>49,51,52</sup> In general, β-scission reactions are more likely than hydrogen transfer reactions during thermal cracking of hydrocarbons, explaining the higher concentration of olefins compared to paraffins.<sup>45</sup> Cleavage of C–C and CH– bonds occurred to produce olefins and diolefins. High concentrations of α-olefins were expected, as chain scission occurs near double bonds. Rescission of α-olefins resulted in α,ω-diolefins as prevalent products.<sup>12</sup> TOD of HDPE also produced an oil with high concentrations of olefins, with lower concentrations of diolefins and paraffins. The concentrations of these hydrocarbon functional groups were not statistically different for pyrolysis and TOD runs at either ER. Furthermore, the amount of oxygen in the oil phase from TOD of HDPE was less than 0.2 wt %. The high yield of olefins is especially desirable, as olefins are basic petrochemical building blocks and can be converted to detergents, sanitizers, plastics, lubricants, and other valuable products.<sup>53</sup>

Analysis of oils from pyrolysis and TOD of PP showed high amounts of branched unsaturated hydrocarbons. In particular, oils from PP had high amounts of the C9 olefin, 2,4-dimethylhept-1-tene, which was present in concentrations as high as 25 wt % of oil. The concentration of this molecule is consistent with other studies.<sup>54,55</sup> The mechanism for producing this molecule involves secondary terminal radicals transferred to tertiary hydrocarbon atoms at 3 and 5 positions from the end followed by chain scission.<sup>55</sup> Other molecules produced in high amounts include 1-butyl-2-propyl-cyclopentane and 4,6,8-trimethyl-1-nonene at 4.4 and 5.3 wt % of the oil, respectively. Like the oil produced from TOD of HDPE, less than 0.2 wt % of oxygenated molecules were detected in the oil produced from TOD of PP, thus preserving the hydrocarbon nature of the pyrolysis products.

Figure 6 shows the MW distribution of the oil phases from pyrolysis and TOD of HDPE (Figure 6A) and PP (Figure 6B). Both types of oil exhibit bimodal distributions, typical of oils from thermal depolymerization of polyolefins.<sup>56</sup> For pyrolysis oils of PP, these peaks occur at 220 and 380 g mol $^{-1}$ . For TOD of PP, oils produced at both ERs show peaks near 195 and 245 g mol $^{-1}$ , with very little product above 380 g mol $^{-1}$ . A similar shift toward lower average MWs in TOD oils was observed for HDPE pyrolysis and TOD oils. Like the shift in the MWs of waxes, this shift of the MWs of oils demonstrates the facility of oxygen to accelerate thermal cracking of polyolefins.

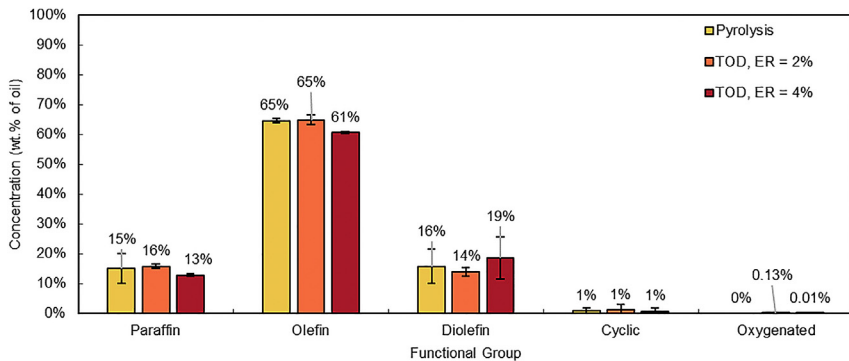


**Figure 5. Oil characterization**

A comparison of oil-phase characterization from pyrolysis of HDPE shows that major hydrocarbon functional groups were preserved during TOD. Error bars represent standard deviation of concentration of oil phases from two trials around the average concentration.

HHVs in the range of 40–43 MJ kg<sup>-1</sup> were found for the oil fraction of products from thermal depolymerization of HDPE and PP (see [supplemental information](#)). One-way ANOVA of these results indicates that the HHV was not significantly influenced by the method of thermal depolymerization for comparable reaction temperature and vapor residence time. Other studies also found HHVs within this range.<sup>57,58</sup> The calorific value of these oils is comparable to that of gasoline and diesel fuel.<sup>59</sup>

One of the most significant takeaways in the comparison of oils produced via pyrolysis and TOD is the similarity of their composition, despite introducing oxygen into the reactor for TOD. Notable was the almost complete absence of oxygenated molecules in the TOD oils. Both pyrolysis and TOD produced hydrocarbons as almost exclusively the products. Accordingly, both pyrolysis and TOD oils can be similarly upgraded. This finding is consistent with the hypothesis of Mayo that oxygen acts as catalysts below 15 vol % oxygen, while higher concentrations produce reactions better characterized as oxidation.<sup>37</sup> For reactions with low oxygen partial pressures, the oxidation rate of hydrocarbons is pressure dependent.<sup>21</sup> The current study supports this hypothesis, as volumetric concentrations of 4 and 7 vol % (ER = 2% and 4%) produced waxes and oils of relatively the same composition as pyrolysis.

TOD offers a route to upcycling plastic wastes to valuable chemicals while dramatically reducing the external energy demand of pyrolysis. Because of the varied enthalpy values generated by use of benchtop systems, it was necessary to first determine the enthalpy for pyrolysis using a system representative of a commercial processing plant. For HDPE and PP at a reaction temperature of 600°C, the enthalpies for pyrolysis were found to be 2,300 ± 90 and 2,800 ± 60 J g<sup>-1</sup>, respectively. During pyrolysis, the thermal energy for devolatilization must be applied by external heat supply. However, TOD was shown to decrease the external energy needed for pyrolysis by up to 85% due to the exothermicity of internal partial oxidation reactions. Furthermore, minimal carbon was sacrificed during TOD to provide this energy. The results of this study demonstrate an increase in oil yields for TOD compared to conventional pyrolysis due to the catalytic effect of oxygen on cracking. The oxygen admitted to TOD primarily ended up in produced water and carbon oxides. Importantly, TOD preserves the composition of the condensable oil containing high concentrations of olefins. This suggests that TOD oil can be upgraded in the same manner as pyrolysis oil. Our work demonstrates that TOD can be deployed for energy-efficient plastic upcycling.

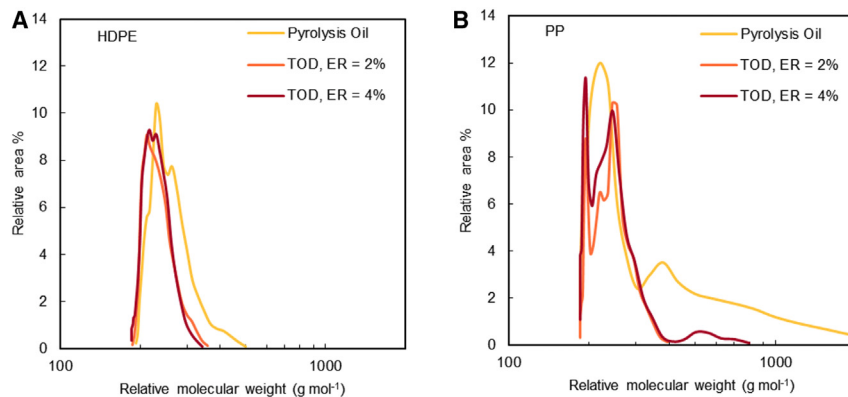


**Figure 6. Oil molecular weight distribution**

GPC chromatograms of the oil phases from pyrolysis and TOD of HDPE (A) and PP (B), with the TOD oils at ERs of 2% and 4%.

## EXPERIMENTAL PROCEDURES

### Resource availability

#### Lead contact

Further information and requests for resources should be directed to and will be fulfilled by the lead contact, Tannon Daugaard ([daugaard@iastate.edu](mailto:daugaard@iastate.edu)).

#### Materials availability

Further information and requests for resources and materials should be directed to and will be fulfilled by the [lead contact](#), Tannon Daugaard ([daugaard@iastate.edu](mailto:daugaard@iastate.edu)).

#### Data and code availability

The original data supporting the current study are available from the [lead contact](#) on request.

### Feedstock preparation and characterization

The plastics used in this study were virgin or first-pass HDPE pellets and virgin or first-pass PP pellets procured from Advanced Production Systems (Cincinnati, OH, USA). These spherical pellets measured approximately 3–5 mm in diameter. The  $M_n$  and  $M_w$  values were obtained using high-temperature gel permeation chromatography (HT-GPC) in a Malvern (Westborough, MA, USA) high-performance liquid chromatography system. Samples of 15–25 mg were dissolved in 1,2,4-trichlorobenzene containing 250 mg L<sup>-1</sup> of 2,6-di-tert-butyl-4-methylphenol as an antioxidant. To ensure complete dissolution, these mixtures were heated to 165°C for 4 h without constant agitation. Samples were analyzed using an Agilent PL-GPC 220 Integrated HT-GPC (Agilent Technologies, Santa Clara, CA, USA) equipped with refractive index (RI) and viscometer detectors. Chromatographic separation occurred using a flow rate of 1.0 mL min<sup>-1</sup> and an oven temperature of 165°C using two PLgel Olexis columns (300 × 7.5 mm) and one PLgel 10 μm 100 Å (300 × 7.5 mm) column in series with MW limits of 0–10,000,000 Da. A calibration curve was obtained using narrow polystyrene standards from 162 to 1,069,000 Da (Agilent Technologies) and converted for use with PE and PP using Mark-Houwink constants, as described in ASTM D6474-20.<sup>60</sup> Data analysis was conducted using Agilent GPC/SEC Software v.2.2 (Agilent Technologies). HHVs were measured using a bomb calorimeter (Parr Instruments 6400 series). MW results and HHVs are presented in [Table 3](#).

**Table 3. Feedstock properties**

	HDPE	PP
Molecular weight (g mol <sup>-1</sup> )		
M <sub>n</sub>	33,000 ± 1,000	146,000 ± 1,000
M <sub>w</sub>	65,000 ± 1,000	270,000 ± 10,000
Higher heating value (MJ kg <sup>-1</sup> )		
	44 ± 2.6	45 ± 0.9

Properties of virgin high-density polyethylene (HDPE) and polypropylene (PP) feedstock in pyrolysis and thermal oxo-degradation experiments. The number-average molecular weight is represented by M<sub>n</sub>, and the weight-average molecular weight is represented by M<sub>w</sub>. Error represents standard deviation of two trials around the average.

### Fluidized bed reactor experiments

A laboratory-scale fluidized bed was used to perform pyrolysis and TOD experiments. The system, originally designed to pyrolyze biomass,<sup>61</sup> was modified for the present experiments. Feedstock streams of pure HDPE and pure PP were tested in the pyrolysis system.

As illustrated in Figure 7, the reactor system consisted of an injection auger, plenum, fluidized bed, and condenser train. The injection auger continuously fed plastic into the fluidized bed. The reactor was a 3.8 cm diameter, 316 stainless-steel pipe containing 250 g silica sand as the bed media. The plenum was heated to 640°C using two 3,000 W Watlow ceramic clam-shell heaters. Fluidizing gas was introduced through the distributor plate at the bottom of the plenum, where it quickly reached operating temperatures, as observed by thermocouples in the plenum and the reactor bed. Thermal energy was provided to the reactor through two 2,100 W Watlow ceramic clam-shell heaters. Proportional-integral-derivative (PID) controllers were used to regulate and monitor reactor temperatures and thermal energy flows. Data logging was provided by OSisoft PI Vision. The product stream exited the fluidized bed reactor through a 12.7 mm transfer line routed to the condenser train. Products were collected using fractional distillation, where the first two stage fractions (SFs) yield waxes and the last two SFs yield liquids. The first stage of the condensate recovery train used a condenser to cool the product stream from 550°C to approximately 130°C, referred to as SF1. SF2 employed an electrostatic precipitator (ESP) operating at 10 kV and 130°C to collect the remainder of the wax. SF3 used a shell-and-tube heat exchanger operated at 0°C to condense liquid products. SF4 used a second ESP operating at 10 kV and -15°C to collect the remainder of the condensable products.

NCGs exiting the condensate recovery train were continuously analyzed using a Varian CP-4900 micro-GC for nitrogen (N<sub>2</sub>), oxygen (O<sub>2</sub>), carbon monoxide (CO), carbon dioxide (CO<sub>2</sub>), hydrogen (H<sub>2</sub>), methane (CH<sub>4</sub>), ethane (C<sub>2</sub>H<sub>6</sub>), ethylene (C<sub>2</sub>H<sub>4</sub>), propane/propylene (C<sub>3</sub>H<sub>8</sub>/C<sub>3</sub>H<sub>6</sub>), and butene (C<sub>4</sub>H<sub>8</sub>). The flow rate of NCGs was determined using a Ritter drum-type gas meter. Gas yields were calculated on a nitrogen- and oxygen-free basis.

During conventional pyrolysis, the devolatilization of plastics to vapor products occurred in an oxygen-free environment. The reactor heaters were used to provide the enthalpy for pyrolysis and overcome parasitic heat losses from the reactor to the surroundings. Parasitic heat losses were determined by holding the fluidized bed at a steady temperature of 600°C while flowing preheated nitrogen through the bed in the absence of plastics feed at a flow rate appropriate to fluidizing the reactor (15.5 L min<sup>-1</sup>). The electric power required to hold the fluidized bed at 600°C represents the

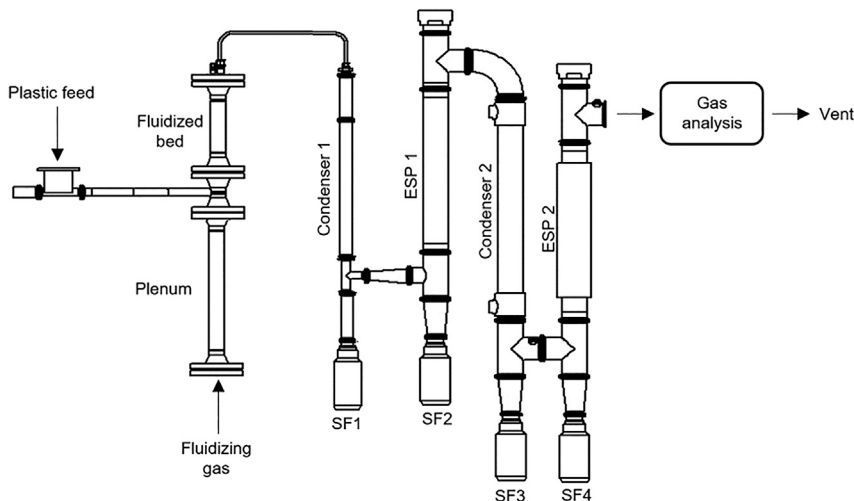


**Figure 7. Reactor system**

Schematic of fluidized bed reactor system used for plastic depolymerization tests.

parasitic heat losses for the reactor at the desired pyrolysis conditions of temperature and gas flow rate. After the baseline electric power to overcome parasitic heat loss was established, experiments began by feeding in plastic pellets at a targeted feed rate of  $600 \text{ g h}^{-1}$  into the reactor and allowing the PID controller to automatically increase electric power to the ceramic heaters enough to maintain the reaction temperature of  $600^\circ\text{C}$ . Reactions were performed for 1 h of continuous feeding. The enthalpy for pyrolysis was calculated by dividing the change in average electric power ( $\text{kJ s}^{-1}$ ) between pyrolysis and parasitic heat loss by the average plastics feed rate ( $\text{kg s}^{-1}$ ).

During TOD, air was introduced into the fluidization gas stream, enabling both devolatilization and partial oxidation of the plastic. TOD was performed at 4 vol % oxygen ( $3 \text{ L min}^{-1}$  air and  $12.5 \text{ L min}^{-1}$  nitrogen) and 7 vol % oxygen ( $4.5 \text{ L min}^{-1}$  air and  $11 \text{ L min}^{-1}$  nitrogen). These conditions correspond to ERs of 2% and 4%, respectively, as calculated using Equation 1. See Table S1 for ER calculations.

$$\text{ER (\%)} = \frac{\dot{m}_{\text{air}}}{\dot{m}_{\text{stoichiometric air}}} \quad (\text{Equation 1})$$

Exothermic oxidation reactions during TOD released heat that decreased the demand for external energy from the ceramic heaters to maintain reactor temperatures. The enthalpy for pyrolysis was calculated by dividing the change in electric power ( $\text{kJ s}^{-1}$ ) between TOD and parasitic heat loss by the plastic feed rate ( $\text{kg s}^{-1}$ ). This methodology is similar to that described in Polin et al.,<sup>30</sup> which determined the ER required to achieve autothermal pyrolysis of biomass.

Product yields and composition were determined for both conventional pyrolysis and TOD experiments at ERs of 2% and 4%. All experiments were performed in duplicate. Yields of wax and liquid products were determined gravimetrically on a plastics feedstock basis, subtracting the weight of oxygen arising from partial oxidation. Thus, product yields greater than 100 wt % were possible, as air was excluded as a reactant. Error bars were generated using the standard deviation of the duplicate trials. Total mass closures exceeded 85 wt % on a fed plastic basis for all pyrolysis and TOD trials.

### Product analyses

Preliminary analyses showed the composition of the wax fractions (SF1 and SF2) to be almost identical; thus, for reporting purposes, the data from these fractions are combined and referred to as wax. Similarly, the liquid fractions (SF3 and SF4) were combined. As liquid products from TOD tests tended to phase separate, a separatory funnel was used to recover these two distinct phases. These phases were referred to as "oil" and "aqueous phase" to distinguish them. See [Figure S1](#) for a schematic detailing the separation and analyses of products.

The MW distribution of pyrolysis and TOD waxes was determined using HT-GPC, which was also used to analyze the feedstock plastics.<sup>62</sup> Refer to [feedstock preparation and characterization](#) for methodology of HT-GPC.

The MW distributions of oil phases were determined using GPC. Samples were dissolved in tetrahydrofuran (THF) and analyzed using a Dionex Ultimate 3000 high-performance liquid chromatograph. THF was used as the mobile phase, and one MesoPore column (3 µm inner diameter, 300 × 7.5 mm; 200–25,000 Da) and two Agilent PLgel columns (3 µm inner diameter, 300 × 7.5 mm; 100–4,000 Da) were used in series. A Shodex RI and diode array detector were used for measurement. Polystyrene standards were used for calibration.

Elemental analysis for carbon and hydrogen concentrations was performed using a vario MICRO cube Elementar Analyzer. Samples of approximately 5 mg were weighed in aluminum boats. The standard used was PE organic analytical standard (Elementar Americas, Ronkonkoma, NY, USA). Tungsten oxide was used as a combustion aid. Oxygen concentration was directly determined using a FlashSmart 2000 Combustion Elemental Analyzer (Thermo Fisher Scientific, Waltham, MA, USA). Silver capsules were baked overnight to remove oxides before samples of approximately ~2.5 mg were weighed in capsules. The standard used was 25-(bis(5-tert-butyl-2-benzo-oxazol-2-yl) thiophene purchased from Elementar Americas. The expected accuracy of the elemental analysis measurements is ±0.3%. All samples were prepared in triplicates.

The oil and aqueous phases were analyzed for concentration of individual compounds using GC-MS/FID with a Polyarc reactor (Activated Research Company). The characterization was performed with an Agilent 5975C GC/MSD (gas chromatograph/mass selective detector) coupled to an Agilent 7890 GC connected with a Polyarc reactor and FID in sequence. A polar-phase Phenomenex DB-1701 fused silica capillary column (60 m × 0.25 mm ID, 0.25 µm film thickness) was used. The GC injector was held at 280°C with helium as the carrier gas with a constant flow of 2 mL min<sup>-1</sup>. The GC oven was programmed to start and hold at 35°C for 3 min and then heat up to 280°C at a rate of 4°C min<sup>-1</sup> and held for 4 min. The MS was operated with electron impact ionization at 280°C with mass-to-charge ratio values recorded over a range of 35–650 m/z. Mass spectral peaks were identified using the NIST 2020 library. The use of a Polyarc reactor in series with a FID allowed for accurate quantification using an internal standard in samples.<sup>63</sup> The internal standard 1-dodecanol was used, as its elution time was distinct from those of compounds present in the sample. Oil samples were prepared by dilution in n-hexane at a ratio of 1:10 w/w.

HHVs for oil phases were measured using a bomb calorimeter (Parr Instruments 6400 series) and are presented in [Table S2](#). Approximately 0.10 g sample was ignited under pressurized oxygen conditions to undergo combustion, and an increase in water bath temperature was recorded to calculate the sample's HHV (MJ kg<sup>-1</sup>). Benzoic

acid was used to verify the working condition of the instrument. Duplicates were performed for each sample.

The moisture content of the aqueous phase obtained during TOD was determined using Karl Fischer titration (Mettler Toledo V30S Compact Volumetric KF Titrator). Three blank samples were run to account for ambient humidity. Approximately 30–60 mg liquid was measured into 10 mL vials and capped. Sample vials were placed in an oven autosampler, where vials were individually heated to 120°C to evaporate water content. Dry air transferred water vapor to the titration vessel, and the resulting solution was titrated using Hydralan 5-K composite titrant. The moisture content of each sample was reported on a weight percentage by the instrument. Duplicates were performed for each sample.

## SUPPLEMENTAL INFORMATION

Supplemental information can be found online at <https://doi.org/10.1016/j.xcrp.2024.101856>.

## ACKNOWLEDGMENTS

This material is based upon work supported by the US Department of Energy, Office of Energy Efficiency and Renewable Energy, Bioenergy Technologies Office, under award number DEEE0009285. The authors would also like to thank the contributions of Patrick Johnston, Lysle Whitmer, Maxwell Beck, Celia Abolafia, Jarrod Long, Maeilia Dzeidzic, Nathan Patel, and Matthew Beard for providing experimental and analytical support of the project. Purchase of the PerkinElmer 2100 Series II CHN/S analyzer used to obtain oxygen elemental analysis results included in this publication was supported in part by the National Science Foundation under grant no. DBI 9413969. We wish to thank Iowa State University Chemical Instrumentation Facility staff members Dr. Sarah Cady and Kaitlyn Bennet for assistance pertaining to the elemental analysis results included in this publication.

## AUTHOR CONTRIBUTIONS

J.L.B., T.J.D., and R.C.B. conceptualized the manuscript. J.L.B. and T.J.D. developed the TOD and pyrolysis methodology. J.L.B., V.S.C., and T.J.D. performed product data curation and analysis. R.G.S. and K.V. provided supervision, project administration, and funding acquisition of the research. J.L.B. wrote the manuscript, with reviewing and editing contributed by all authors.

## DECLARATION OF INTERESTS

The authors declare no competing interests.

Received: November 17, 2023

Revised: January 11, 2024

Accepted: February 13, 2024

Published: March 8, 2024

## REFERENCES

1. Geyer, R., Jambeck, J.R., and Law, K.L. (2017). Production, use, and fate of all plastics ever made. *Sci. Adv.* 3, 1700782–e1700829. <https://doi.org/10.1126/sciadv.1700782>.
2. Li, H., Aguirre-Villegas, H.A., Allen, R.D., Bai, X., Benson, C.H., Beckham, G.T., Bradshaw, S.L., Brown, J.L., Brown, R.C., Cecon, V.S., et al. (2022). Expanding plastics recycling technologies: chemical aspects, technology status and challenges. Preprint at Royal Society of Chemistry. <https://doi.org/10.1039/d2gc02588d>.
3. Buekens, A. (2006). Introduction to Feedstock Recycling of Plastics. In *Feedstock Recycling and Pyrolysis of Waste Plastics: Converting Waste Plastics into Diesel and Other Fuels*, W. Schiers, John, and Kaminsky, eds. (John Wiley & Sons, Ltd)), pp. 1–41. <https://doi.org/10.1002/0470021543.ch1>.
4. Lopez, G., Artetxe, M., Amutio, M., Bilbao, J., and Olazar, M. (2017). Thermochemical routes

- for the valorization of waste polyolefinic plastics to produce fuels and chemicals. A review. *Renew. Sustain. Energy Rev.* 73, 346–368. <https://doi.org/10.1016/j.rser.2017.01.142>.
5. Zhao, D., Wang, X., Miller, J.B., and Huber, G.W. (2020). The Chemistry and Kinetics of Polyethylene Pyrolysis: A Process to Produce Fuels and Chemicals. *ChemSusChem* 13, 1764–1774. <https://doi.org/10.1002/cssc.201903434>.
  6. Zhang, Y., Fu, Z., Wang, W., Ji, G., Zhao, M., and Li, A. (2022). Kinetics, Product Evolution, and Mechanism for the Pyrolysis of Typical Plastic Waste. *ACS Sustain. Chem. Eng.* 10, 91–103. <https://doi.org/10.1021/acssuschemeng.1c04915>.
  7. Orozco, S., Alvarez, J., Lopez, G., Artetxe, M., Bilbao, J., and Olazar, M. (2021). Pyrolysis of plastic wastes in a fountain confined conical spouted bed reactor: Determination of stable operating conditions. *Energy Convers. Manag.* 229, 113768. <https://doi.org/10.1016/j.enconman.2020.113768>.
  8. Sogancioglu, M., Ahmetli, G., and Yel, E. (2017). A Comparative Study on Waste Plastics Pyrolysis Liquid Products Quantity and Energy Recovery Potential. *Energy Proc.* 118, 221–226. <https://doi.org/10.1016/j.egypro.2017.07.020>.
  9. Singh, R.K., and Ruj, B. (2016). Time and temperature depended fuel gas generation from pyrolysis of real world municipal plastic waste. *Fuel* 174, 164–171. <https://doi.org/10.1016/j.fuel.2016.01.049>.
  10. Sikdar, S., Siddaiah, A., and Menezes, P.L. (2020). Conversion of waste plastic to oils for tribological applications. *Lubricants* 8, 78. <https://doi.org/10.3390/LUBRICANTS800078>.
  11. Rodríguez, E., Gutiérrez, A., Palos, R., Vela, F.J., Arandes, J.M., and Bilbao, J. (2019). Fuel production by cracking of polyolefins pyrolysis waxes under fluid catalytic cracking (FCC) operating conditions. *Waste Manag.* 93, 162–172. <https://doi.org/10.1016/j.wasman.2019.05.005>.
  12. Abbas-Abadi, M.S., Ureel, Y., Eschenbacher, A., Vermeire, F.H., Varghese, R.J., Oenema, J., Stefanidis, G.D., and Van Geem, K.M. (2023). Challenges and opportunities of light olefin production via thermal and catalytic pyrolysis of end-of-life polyolefins: Towards full recyclability. *Prog. Energy Combust. Sci.* 96, 101046. <https://doi.org/10.1016/j.pecs.2022.101046>.
  13. Sharma, B.K., Moser, B.R., Vermillion, K.E., Doll, K.M., and Rajagopalan, N. (2014). Production, characterization and fuel properties of alternative diesel fuel from pyrolysis of waste plastic grocery bags. *Fuel Process. Technol.* 122, 79–90. <https://doi.org/10.1016/j.fuproc.2014.01.019>.
  14. Predel, M., and Kaminsky, W. (2000). Pyrolysis of mixed polyolefins in a fluidized-bed reactor and on a pyro-GC/MS to yield aliphatic waxes. *Polym. Degrad. Stabil.* 70, 373–385. [https://doi.org/10.1016/S0141-3910\(00\)00131-2](https://doi.org/10.1016/S0141-3910(00)00131-2).
  15. Bui, V.T., Khuong, T.H., Bui, V.H., Le, T.H., and Pham, V.V. (2021). A Review On The Use Of Plastic Waste-Originated Fuels For
  - Compression Ignition Engines. *Journal of Mechanical Engineering Research and Developments* 44, 43–54.
  16. Punkkinen, H., Oasmaa, A., Laatikainen-Luntama, J., Nieminen, M., and Laine-Ylijoki, J. (2017). Thermal Conversion of Plastic-Containing Waste: A Review.
  17. Elordi, G., Arabiourrutia, M., Bilbao, J., and Olazar, M. (2018). Energetic Viability of a Polyolefin Pyrolysis Plant. *Energy Fuels* 32, 3751–3759. <https://doi.org/10.1021/acs.energyfuels.7b03664>.
  18. Zhang, Y., Ji, G., Ma, D., Chen, C., Wang, Y., Wang, W., and Li, A. (2020). Exergy and energy analysis of pyrolysis of plastic wastes in rotary kiln with heat carrier. *Process Saf. Environ. Protect.* 142, 203–211. <https://doi.org/10.1016/j.psep.2020.06.021>.
  19. Brown, R.C. (2020). Process Intensification through Directly Coupled Autothermal Operation of Chemical Reactors. *Joule* 4, 2268–2289. <https://doi.org/10.1016/j.joule.2020.09.006>.
  20. Peterson, J.D., Vyazovkin, S., and Wight, C.A. (2001). Kinetics of the thermal and thermo-oxidative degradation of polystyrene, polyethylene and poly(propylene). *Macromol. Chem. Phys.* 202, 775–784. [https://doi.org/10.1002/1521-3935\(20010301\)202:6<775::AID-MACP775>3.0.CO;2-G](https://doi.org/10.1002/1521-3935(20010301)202:6<775::AID-MACP775>3.0.CO;2-G).
  21. Grassie, N., and Scott, G. (1985). *Polymer Degradation and Stabilisation* (Cambridge University Press).
  22. Alam, T.M., Celina, M., Assink, R.A., Clough, R.L., Gillen, K.T., and Wheeler, D.R. (2000). Investigation of oxidative degradation in polymers using <sup>17</sup>O NMR spectroscopy. *Macromolecules* 33, 1181–1190. <https://doi.org/10.1021/ma991061o>.
  23. Koç, A., and Bilgesü, A.Y. (2007). Catalytic and thermal oxidative pyrolysis of LDPE in a continuous reactor system. *J. Anal. Appl. Pyrolysis* 78, 7–13. <https://doi.org/10.1016/j.jaap.2006.03.008>.
  24. Salaudeen, S.A., Arku, P., and Dutta, A. (2018). Gasification of plastic solid waste and competitive technologies. In *Plastics to Energy: Fuel, Chemicals, and Sustainability Implications*, pp. 269–293. <https://doi.org/10.1016/B978-0-12-813140-4.00010-8>.
  25. Ciuffi, B., Chiaramonti, D., Rizzo, A.M., Frediani, M., and Rosi, L. (2020). A critical review of SCWG in the context of available gasification technologies for plastic waste. *Appl. Sci.* 10, 6307. <https://doi.org/10.3390/APP10186307>.
  26. Brown, R.C. (2021). The Role of Pyrolysis and Gasification in a Carbon Negative Economy. *Processes* 9, 882.
  27. Brems, A., Dewil, R., Baeyens, J., and Zhang, R. (2015). Gasification of Plastic Waste as Waste-to-Energy or Waste-to-Syngas Recovery Route. In *Solid Waste as a Renewable Resource: Methodologies* (Apple Academic Press), pp. 241–264. <https://doi.org/10.4236/ns.2013.56086>.
  28. Mastral, F.J., Esperanza, E., Berrueto, C., Juste, M., and Ceamanos, J. (2003). Fluidized bed thermal degradation products of HDPE in an inert atmosphere and in air-nitrogen mixtures. *J. Anal. Appl. Pyrolysis* 70, 1–17. [https://doi.org/10.1016/S0165-2370\(02\)00068-2](https://doi.org/10.1016/S0165-2370(02)00068-2).
  29. Polin, J.P., Carr, H.D., Whitmer, L.E., Smith, R.G., and Brown, R.C. (2019). Conventional and autothermal pyrolysis of corn stover: Overcoming the processing challenges of high-ash agricultural residues. *J. Anal. Appl. Pyrolysis* 143, 104679.
  30. Polin, J.P., Peterson, C.A., Whitmer, L.E., Smith, R.G., and Brown, R.C. (2019). Process intensification of biomass fast pyrolysis through autothermal operation of a fluidized bed reactor. *Appl. Energy* 249, 276–285. <https://doi.org/10.1016/j.apenergy.2019.04.154>.
  31. Daugaard, D.E., and Brown, R.C. (2003). Enthalpy for pyrolysis for several types of biomass. *Energy Fuels* 17, 934–939. <https://doi.org/10.1021/ef020260x>.
  32. Duque, J.V.F., Martins, M.F., Debenest, G., and Orlando, M.T.D. (2020). The influence of the recycling stress history on LDPE waste pyrolysis. *Polym. Test.* 86, 106460. <https://doi.org/10.1016/j.polymertesting.2020.106460>.
  33. Khedri, S., and Elyasi, S. (2018). Determination of the heat of pyrolysis of HDPE via isothermal differential scanning calorimetry: A new approach for solid state reactions. *J. Therm. Anal. Calorim.* 131, 1509–1515. <https://doi.org/10.1007/s10973-017-6681-x>.
  34. Agarwal, G., and Lattimer, B. (2012). Method for measuring the standard heat of decomposition of materials. *Thermochim. Acta* 545, 34–47. <https://doi.org/10.1016/j.tca.2012.06.027>.
  35. Elordi, G., Olazar, M., Aguado, R., Lopez, G., Arabiourrutia, M., and Bilbao, J. (2007). Catalytic pyrolysis of high density polyethylene in a conical spouted bed reactor. *J. Anal. Appl. Pyrolysis* 79, 450–455. <https://doi.org/10.1016/j.jaap.2006.11.010>.
  36. Westerhout, R.W.J., Van Koningsbruggen, M.P., Van Der Ham, A.G.J., Kuipers, J.A.M., and Van Swaaij, W.P.M. (1998). Techno-economic evaluation of high temperature pyrolysis processes for mixed plastic waste. *Chem. Eng. Res. Des.* 76, 427–439. <https://doi.org/10.1205/026387698524857>.
  37. Mayo, F.R. (1976). Oxidation Induced Pyrolyses of Plastics. *J. Polym. Sci. B. Polym. Lett. Ed.* 14, 713–716.
  38. Dispons, J. (2006). Continuous Thermal Process for Cracking Polyolefin Wastes to Produce Hydrocarbons. In *Feedstock Recycling and Pyrolysis of Waste Plastics: Converting Waste Plastics into Diesel and Other Fuels*, Schiers, John and W. Kaminsky, eds. (John Wiley & Sons, Ltd)), pp. 595–604.
  39. Cunliffe, A.M., and Williams, P.T. (1998). Composition of oils derived from the batch pyrolysis of tyres. *J. Anal. Appl. Pyrolysis* 44, 131–152. [https://doi.org/10.1016/S0165-2370\(97\)00085-5](https://doi.org/10.1016/S0165-2370(97)00085-5).
  40. Arabiourrutia, M., Elordi, G., Olazar, M., and Bilbao, J. (2017). Pyrolysis of Polyolefins in a Conical Spouted Bed Reactor: A Way to Obtain Valuable Products. *Mater. Sci.* 10, 5772/67706.
  41. Arabiourrutia, M., Elordi, G., Lopez, G., Borsella, E., Bilbao, J., and Olazar, M. (2012).

- Characterization of the waxes obtained by the pyrolysis of polyolefin plastics in a conical spouted bed reactor. *J. Anal. Appl. Pyrolysis* 94, 230–237. <https://doi.org/10.1016/j.jaat.2011.12.012>.
42. Dogu, O., Pelucchi, M., Van de Vijver, R., Van Steenberge, P.H., D'hooge, D.R., Cuoci, A., Mehl, M., Frassoldati, A., Faravelli, T., and Van Geem, K.M. (2021). The chemistry of chemical recycling of solid plastic waste via pyrolysis and gasification: State-of-the-art, challenges, and future directions. *Prog. Energy Combust. Sci.* 84, 100901. <https://doi.org/10.1016/j.pecs.2020.100901>.
43. Soják, L., Kubinec, R., Jurdáková, H., Hájeková, E., and Bajus, M. (2007). High resolution gas chromatographic-mass spectrometric analysis of polyethylene and polypropylene thermal cracking products. *J. Anal. Appl. Pyrolysis* 78, 387–399. <https://doi.org/10.1016/j.jaat.2006.09.012>.
44. Allen, N.S. (1983). *Degradation and Stabilization of Polymers* (Applied Science Publishers).
45. Miskolczi, N. (2006). Kinetic Model of the Chemical and Catalytic Recycling of Waste Polyethylene into Fuels. In *Feedstock Recycling and Pyrolysis of Waste Plastics: Converting Waste Plastics into Diesel and Other Fuels*, J. Schiers and W. Kaminsky, eds. (Wiley), pp. 225–247. <https://doi.org/10.1002/0470021543.ch9>.
46. Câmara, L.D.T., Furtado, N.C., Monteiro, R.S., Aranda, D.A., and Taft, C.A. (2006). Molecular orbital approach for investigating the kinetics of cracking hydroperoxides. *J. Mol. Struct.: THEOCHEM* 776, 41–45. <https://doi.org/10.1016/j.theochem.2006.08.024>.
47. Al-Salem, S.M., and Dutta, A. (2021). Wax Recovery from the Pyrolysis of Virgin and Waste Plastics. *Ind. Eng. Chem. Res.* 60, 8301–8309. <https://doi.org/10.1021/acs.iecr.1c01176>.
48. Aguado, R., Olazar, M., San José, M.J., Gaisán, B., and Bilbao, J. (2002). Wax formation in the pyrolysis of polyolefins in a conical spouted bed reactor. *Energy Fuels* 16, 1429–1437. <https://doi.org/10.1021/ef020043w>.
49. Miskolczi, N., Bartha, L., Deák, G., and Jóver, B. (2004). Thermal degradation of municipal plastic waste for production of fuel-like hydrocarbons. *Polym. Degrad. Stabil.* 86, 357–366. <https://doi.org/10.1016/j.polymdegradstab.2004.04.025>.
50. Aguado, R., Olazar, M., Gaisán, B., Prieto, R., and Bilbao, J. (2002). Kinetic study of polyolefin pyrolysis in a conical spouted bed reactor. *Ind. Eng. Chem. Res.* 41, 4559–4566. <https://doi.org/10.1021/ie0201260>.
51. Conesa, J.A., Font, R., and Marcilla, A. (1997). *Comparison between the Pyrolysis of Two Types of Polyethylenes in a Fluidized Bed Reactor*.
52. Jaafar, Y., Abdelouahed, L., Hage, R.E., Taouk, B., Samrani, A.E., and Taouk, B. (2022). Pyrolysis of common plastics and their mixtures to produce valuable petroleum-like products. *Polym. Degrad. Stabil.* 195, 109770. <https://doi.org/10.1016/j.polymdegradstab.2021.109770>.
53. Borland, J.E., Carroll, G.T., Dighton, G.L., Hu, P.C., Koski, C.L., Lam, W.Y., Lappin, G.R., Okumura, O., Paul, D., Perozzi, E.F., et al. (1989). In *Alpha olefins applications handbook*, G.R. Lappin and J.D. Sauer, eds. (Marcel Dekker, Inc.).
54. Scheirs, J. (2006). Overview of Commercial Pyrolysis Processes for Waste Plastics. In *Feedstock Recycling and Pyrolysis of Waste Plastics: Converting Waste Plastics into Diesel and Other Fuels*, J. Schiers and W. Kaminsky, eds. (John Wiley & Sons), pp. 381–433. <https://doi.org/10.1002/0470021543.ch15>.
55. De Amorim, M.P., Comel, C., and Vermande, P. (1982). Pyrolysis of Polypropylene I. Identification of Compounds and Degradation Reactions. *J. Anal. Appl. Pyrolysis* 4, 73–81.
56. Williams, P.T. (2006). Yield and Composition of Gases and Oils/Waxes from the Feedstock Recycling of Waste Plastic. In *Feedstock Recycling and Pyrolysis of Waste Plastics: Converting Waste Plastics into Diesel and Other Fuels*, J. Schiers and W. Kaminsky, eds. (John Wiley & Sons), pp. 285–313. <https://doi.org/10.1002/0470021543.ch11>.
57. Ahmad, I., Khan, M.I., Khan, H., Ishaq, M., Tariq, R., Gul, K., and Ahmad, W. (2015). Pyrolysis study of polypropylene and polyethylene into premium oil products. *Int. J. Green Energy* 12, 663–671. <https://doi.org/10.1080/1543505.2014.880146>.
58. Quesada, L., Calero, M., Martín-Lara, M.Á., Pérez, A., and Blázquez, G. (2020). Production of an Alternative Fuel by Pyrolysis of Plastic Wastes Mixtures. *Energy Fuels* 34, 1781–1790. <https://doi.org/10.1021/acs.energyfuels.9b03350>.
59. Shakirullah, M., Ahmad, W., Ahmad, I., and Ishaq, M. (2010). Oxidative desulphurization study of gasoline and kerosene role of some organic and inorganic oxidants. *Fuel Process. Technol.* 91, 1736–1741. <https://doi.org/10.1016/j.fuproc.2010.07.014>.
60. International, A. (2020). ASTM D6474-20, Standard test method for determining molecular weight distribution and molecular weight averages of polyolefins by high temperature gel permeation chromatography.
61. Rollag, S.A., Lindstrom, J.K., and Brown, R.C. (2020). Pretreatments for the continuous production of pyrolytic sugar from lignocellulosic biomass. *Chem. Eng. J.* 385, 123889. <https://doi.org/10.1016/j.cej.2019.123889>.
62. Cecon, V.S., Curtzwiler, G.W., and Vorst, K.L. (2022). A Study on Recycled Polymers Recovered from Multilayer Plastic Packaging Films by Solvent-Targeted Recovery and Precipitation (STRAP). *Macromol. Mater. Eng.* 307. <https://doi.org/10.1002/mame.202200346>.
63. Bai, L., Carlton, D.D., and Schug, K.A. (2018). Complex mixture quantification without calibration using gas chromatography and a comprehensive carbon reactor in conjunction with flame ionization detection. *J. Separ. Sci.* 41, 4031–4037. <https://doi.org/10.1002/jssc.201800383>.